doi:10.2109/jcersj2.16255

High thermal-stability ceria synthesized via thermal-hydrolysis route and methane-combustion performance

Naotaka OHTAKE, Masahiro KATOH[*] and Shigeru SUGIYAMA[*,]**

Department of Chemical Science and Technology, Graduate School of Advanced Technology and Science, Tokushima University, Minamijosanjima, Tokushima 770–8506, Japan
[*]Department of Applied Chemistry, Graduate School of Science and Technology, Tokushima University, Minamijosanjima, Tokushima 770–8506, Japan
[**]Department of Resource Circulation Engineering, Center for Frontier Research of Engineering, Tokushima University, Minamijosanjima, Tokushima 770–8506, Japan

Journal of the Ceramic Society of Japan 125 [2] 57-61 2017 Reprint

第125巻　第２号　平成29年２月１日発行（毎月1回1日発行）　ISSN 1348-6535 CODEN: JCSJEW

JCS-Japan

February

vol.125

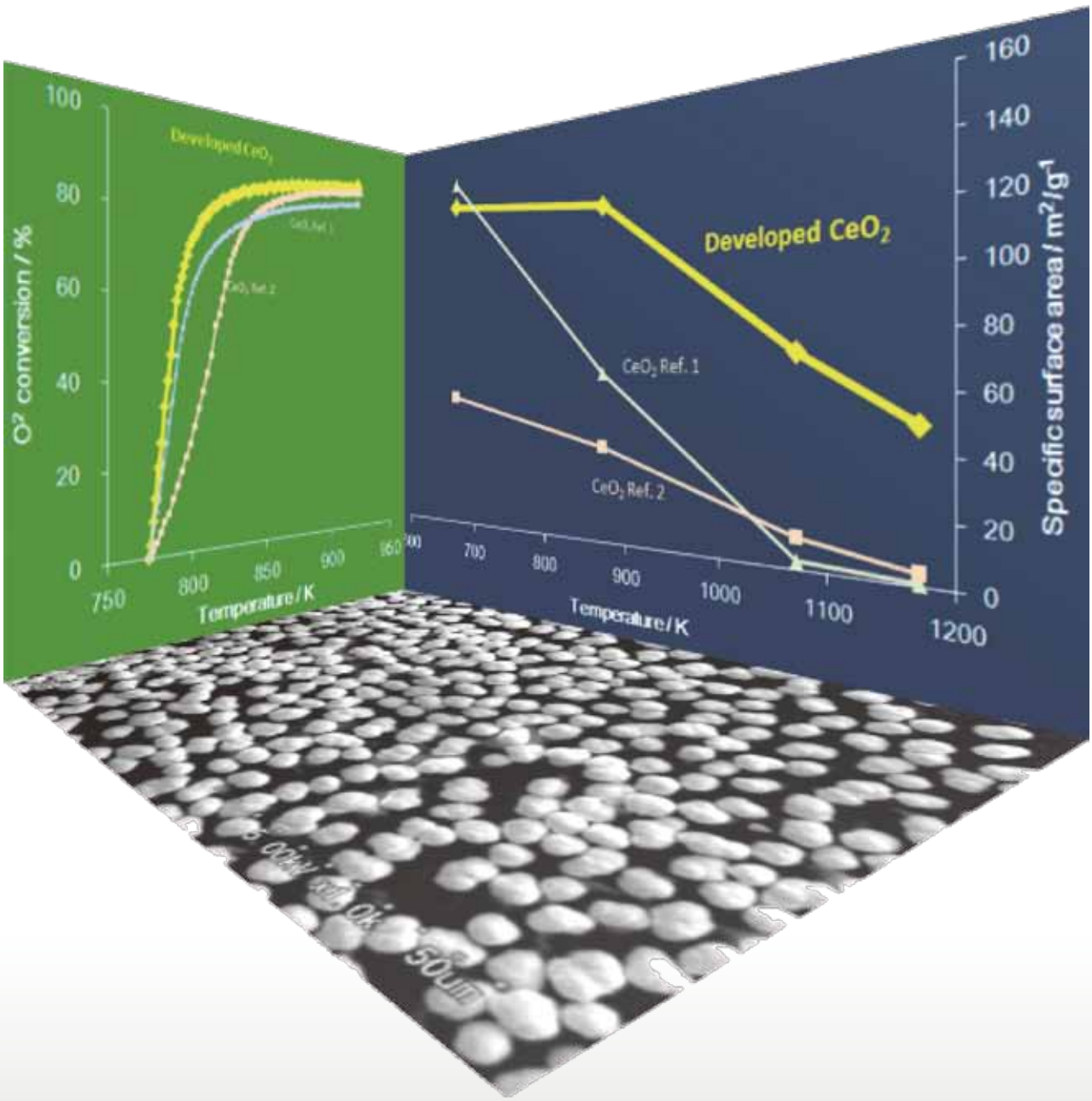

Journal of the Ceramic Society of Japan

2017

Journal of the Ceramic Society of Japan 125 [2] 57-61 2017 Full paper

High thermal-stability ceria synthesized via thermal-hydrolysis route and methane-combustion performance

Naotaka OHTAKE, Masahiro KATOH* and Shigeru SUGIYAMA*,,†**

Department of Chemical Science and Technology, Graduate School of Advanced Technology and Science, Tokushima University, Minamijosanjima, Tokushima 770–8506, Japan

***Department of Applied Chemistry, Graduate School of Science and Technology, Tokushima University, Minamijosanjima, Tokushima 770–8506, Japan**

****Department of Resource Circulation Engineering, Center for Frontier Research of Engineering, Tokushima University, Minamijosanjima, Tokushima 770–8506, Japan**

Enhancement of the thermal stability of a catalyst is an efficient way to improve the catalytic activity of a catalytic reaction performed at high temperature. In this study, cerium oxide (ceria, CeO_2) with a high thermal stability was synthesized by controlling the agglomeration of the primary particles via the thermal hydrolysis of ceric nitrate, accompanied by testing for the catalytic combustion of methane (CH_4). The specific surface area of this material after calcination at 1,173 K for 5 h was 50 m^2/g, which was much higher than that of the two reference materials (ceria made via precipitation of cerous nitrate using aqueous ammonia at 4.1 m^2/g, and the Japan reference catalyst JRC-CEO-1 at 1.4 m^2/g). The ceria made via thermal hydrolysis showed high crystallinity and a much higher pore volume, which resulted in excellent thermal resistance. For O_2 conversion in ceria, catalyzed CH_4 combustion at 923 K, the ceria created in this study demonstrated higher activity than that for either reference. The high CH_4 combustion performance was due to the high specific surface area and to a superior oxygen storage capacity (OSC) even after a combustion test.

Key-words : Cerium oxide, Thermal hydrolysis, Thermal stability, Catalytic combustion, Methane

[Received November 2, 2016; Accepted November 26, 2016]

1. Introduction

Catalysts are widely used in chemical applications such as environmental purification, material synthesis and energy conversion in order to comply with regulations, to reduce production costs, and to synthesize particular products. The development of useful catalysts via a combination of chemical composition and morphology control has been continuously studied. Computing chemical engineering methods is effectively in determining fundamentals of a chemical reaction on a catalyst followed by a designation of the catalyst, which results in better catalytic performance.[1] Ceria, CeO_2, is a unique catalyst with characteristic properties that include a high oxygen storage performance associated with the valence change between Ce^{3+} and Ce^{4+}, a surface charge with high basicity and weak acidity, and a high level of crystal-phase stability.[2)–5)]

The catalytic activity of ceria strongly depends on its physical properties. The modification of primary particle properties such as crystal structure, crystal shape, crystal size, and overall crystallinity are key influential properties.[6),7)] Other physical properties that are related to the agglomeration of primary particles such as specific surface area, porosity, and particle size distribution are also important factors. To maximize catalytic performance, these properties should be controlled with consideration given to the designed chemical reaction, the reaction conditions such as gas atmosphere and temperature, and the reaction device.

In some applications using a catalyst such as the catalytic combustion of organic materials, the reaction is performed at high temperatures higher than 873 K. When ceria catalyst is used in a catalytic reaction performed at high temperature, the primary particles of the ceria are sintered by heating, which results in a subsequent loss of the specific surface area with a concomitant decrease in the catalytic performance. To address this challenge, several synthesis routes for ceria with high thermal stability have been studied. Bruce et al. synthesized ceria via the precipitation of $(NH_4)_2[Ce(NO_3)_6]$ with ammonium carbonate under a CO_2 gas flow. The specific surface area after calcination at 873 K for 2 h was as high as 200 m^2/g.[8)] Kamimura et al. made mesoporous ceria by simple template-free precipitation using $Ce(NO_3)_3$ and NaOH. This oxide had a specific surface area of 21 m^2/g after calcination at 823 K for 10 h.[9)] Terribile et al. prepared hydrous cerium oxide via a surfactant-assisted route. The ceria obtained by calcination of the precursor at 1,173 K for at least 2 h showed ca. 40 m^2/g.[10)]

In the present study, ceria with high thermal stability was synthesized via the thermal hydrolysis of ceric nitrate without the use of organic additives in order to produce a product that would be suitable for simple and safe mass production. The catalytic performance of the synthesized ceria was evaluated by methane combustion at 923 K to establish its high thermal stability. The ceria was characterized using various techniques that included porosity, XRD, H_2-TPR, and BET specific surface area.

2. Experimental procedures

2.1 Synthesis and characterization of ceria with high thermal stability

Ceria was prepared via thermal hydrolysis route. 1 L of aqueous solution of ceric nitrate, ($H_x[Ce(NO_3)_{4+x}]$), (Solvay) containing 20 g of CeO_2 was prepared. This solution was heated to

† Corresponding author: S. Sugiyama; E-mail: sugiyama@tokushima-u.ac.jp

DOI http://doi.org/10.2109/jcersj2.16255

393 K to obtain cerium hydroxide suspension and was maintained at this temperature for 2 h. After cooling down of the suspension, aqueous ammonia was introduced to adjust the pH to 8. The obtained slurry was separated using a nutsche filter. The cake thus obtained was calcined at 673 K for 10 h under air to obtain ceria powder. This ceria is denoted HSA Ceria. A reference ceria was prepared via the precipitation of cerous nitrate with basic solution. 0.67 L of aqueous solution of cerous nitrate, $Ce(NO_3)_3$, (Solvay) containing 200 g of CeO_2 was prepared. This solution was introduced to 1.33 L of 3.14 mol/L aqueous ammonia under agitation. The slurry thus obtained was agitated for 30 min, then separated using nutsche filter and washed with deionized water. The cake thus obtained was calcined at 673 K for 10 h under air, then ground in a mortar to obtain ceria powder. This reference ceria is denoted LSA Ceria. A ceria powder (JRC-CEO-1) supplied by the Catalysis Society of Japan was used as a reference.

The specific surface area of the ceria was measured via the BET method using a N_2 isotherm (Macsorb HM model-1220, Mountech Co.). The primary particle size in the (111) plane was calculated with the Scherrer equation utilizing X-ray diffraction (XRD; RINT 2000 using monochromatized Cu Kα radiation (Rigaku Co.)). The pore-size distribution was analyzed via N_2 adsorption–desorption isotherms obtained using a TriStar 3000 (Micromeritics Co.). We used H_2 temperature-programed reduction (H_2-TPR) to evaluate the oxygen storage capacity (OSC) of the ceria. In H_2-TPR, a catalyst (0.1 g) was treated at 773 K for 1 h under an Ar flow. After the temperature was decreased to 473 K, the Ar flow was switched to 10% H_2/Ar (30.0 sccm). The H_2 consumption via the reduction of Ce^{4+} to Ce^{3+} from 473 to 1,073 K at a heating rate of 10 K/min under a 10% H_2/Ar flow (30.0 sccm) was detected by TCD.

2.2 Catalytic activity test

Ceria was used in the catalytic combustion of methane in a fixed-bed continuous flow reactor under atmospheric pressure at 923 K using a BELCAT II (MicrotracBEL Co.). For this reaction, 50 mg of the fresh ceria was pretreated at 773 K for 1 h under an O_2 flow (25.0 sccm). The O_2 flow was then switched to He (17.9 sccm), O_2 (3.6 sccm), and CH_4 (8.5 sccm) at this temperature. The temperature was raised to 923 K at a heating rate of 10 K/min, then ceria-catalyzed methane combustion at 923 K was continued for 270 min. The O_2 conversion was analyzed using a Q-mass detector.

3. Results and discussion

3.1 Characteristics of ceria with high thermal stability

Figure 1 shows a scanning electron microscope (SEM) image of the HSA Ceria powder. This material consisted of spherical and highly mono-dispersed particles. This unique structure was formed by agglomeration of primary particles of cerium hydroxide during thermal treatment at 393 K.

Table 1 summarizes the specific surface areas of fresh ceria and after calcination of the thus-obtained oxide at 873, 1,073, and 1,173 K for 5 h under air. HSA Ceria showed 139 m^2/g at 673 K and maintained a high specific surface area of 50 m^2/g even after calcination at 1,173 K. The two references had different specific surface areas of 55 and 149 m^2/g at 673 K, but these specific surface areas were drastically decreased to single-digits at 1,173 K. The summary shows that only the HSA Ceria had a significantly high level of thermal stability. The highest level obtained in specific surface area for ceria compared to prior arts was 50 m^2/g at 1,173 K.

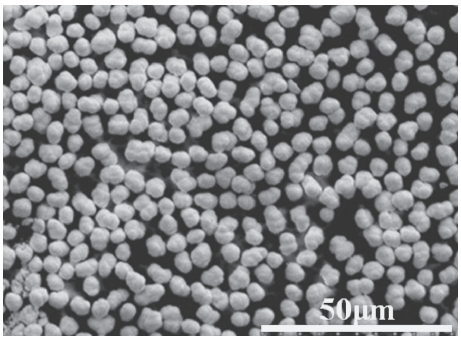

Fig. 1. SEM image of HSA Ceria powder.

Table 1. Specific surface area of ceria with calcination temperature

	Specific surface area/$m^2\,g^{-1}$			
	673 K	873 K	1,073 K	1,173 K
HSA Ceria	139	131	73	50
LSA Ceria	55	37	11	4.1
JRC-CEO-1	149	66	3.5	1.4

Table 2. Primary particle size of ceria in the (111) plane after calcination at 673 and 1,173 K

	Primary particle size/nm	
	673 K	1,173 K
HSA Ceria	9	34
LSA Ceria	13	>100
JRC-CEO-1	7	>100

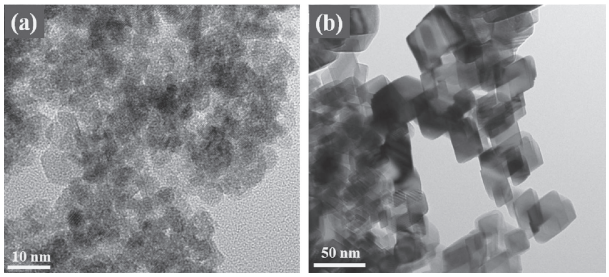

Fig. 2. TEM image of HSA Ceria after calcination at 673 K (a) and 1,173 K (b) under air.

In order to determine the key properties of HSA Ceria that allows the maintenance of a high specific surface area at high temperature, some characterizations were performed making comparisons to the references. **Table 2** gives the primary particle size of ceria in the (111) plane, as detected by XRD. The primary particle size of HSA Ceria calcined at 673 K was 9 nm. After calcination at 1,173 K, the size was kept small at 34 nm, whereas two references showed larger than 100 nm. Therefore, HSA Ceria maintained a smaller primary particle size even after calcination at high temperature.

Figure 2 displays the transmission electron microscope (TEM) images of the fresh HSA Ceria (a) and after calcination at 1,173 K (b). The fresh oxide consisted of 5–10 nm sized primary particles with a highly-crystalline polyhedral-facetted structure. After calcination at 1,173 K, the primary particle size was increased to 25–50 nm and the crystal structure was transferred to that of an octahedral with a (111) surface, which was the most thermodynamically stable structure.[1)] The primary particle size detected by

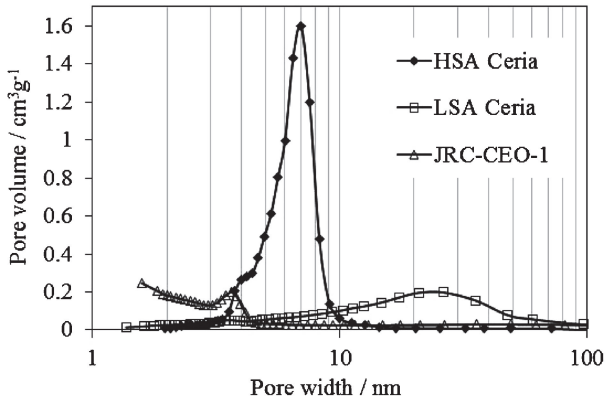

Fig. 3. N_2 pore size distribution of HSA Ceria, LSA Ceria and JRC-CEO-1 after calcination at 673 K under air.

Table 3. Pore volume of pores having no more than 100 nm of ceria after calcination at 673 and 1,173 K

	Pore volume/cm^3 g^{-1}	
	673 K	1,173 K
HSA Ceria	0.30	0.24
LSA Ceria	0.16	<0.01
JRC-CEO-1	0.12	<0.01

XRD showed good agreement with the largest level of particle size observed by TEM. Based on these results, the high specific surface area of HSA Ceria, even after severe ageing, was derived by the prevention of sintering to maintain a small primary particle size. This characteristic phenomenon of HSA Ceria can be explained by the porosity of the oxide. **Figure 3** compares the pore size distribution of ceria obtained by calcination at 673 K for 10 h, while **Table 3** compares the pore volume of pores that are no more than 100 nm in size. The HSA Ceria had a single, and very large, pore size distribution profile with a mean pore size of around 7 nm, and a pore volume of 0.30 cm^3/g that was much higher than that of the reference samples. After calcination at 1,173 K, the pore volume of HSA Ceria was maintained at 0.24 cm^3/g. LSA Ceria consisted of pores with a broad pore size distribution and a mean pore size at around 25 nm. The pore volume of this material was 0.16 cm^3/g, but it was drastically decreased to less than 0.01 cm^3/g at 1,173 K. JRC-CEO-1 had pore sizes in the range of not more than 5 nm and the lowest pore volume of 0.12 cm^3/g. The pore volume after calcination at 1,173 K was less than 0.01 cm^3/g. Therefore, HSA Ceria held a significantly large pore volume with a mean pore size at 7 nm. Since this pore size approximates the primary particle size of 9 nm by XRD or 5–10 nm by TEM, the pores of the HSA Ceria seemed to have originated in the interspaces of mono-dispersed primary particles. If mono-dispersed primary particles are orderly agglomerated, the size of their interfaces might be 0.4 times larger than the primary particle size in a geometric manner. However, in this study, the mean pore size of the HSA Ceria measured via N_2 adsorption–desorption isotherms seemed to be larger than that estimated from the primary particle size. This suggested that the each primary particle of HSA Ceria was connected sparsely to enlarge the pores with concomitant increase in the pore volume. Therefore, this high meso-porous structure provided limited sintering of the primary particles during calcination, which resulted in a high specific surface area even after calcination at high temperature.

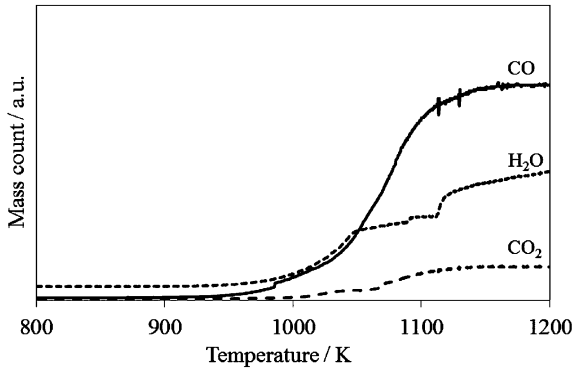

Fig. 4. Temperature programed homogeneous gas phase reaction of CH_4 and O_2.

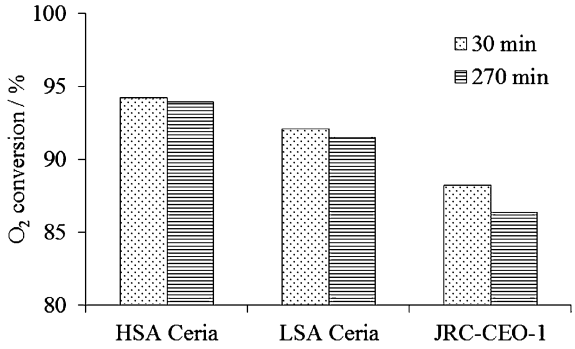

Fig. 5. O_2 conversion after 30 and 270 min of ceria catalyzed CH_4 combustion at 923 K over HSA Ceria, LSA Ceria and JRC-CEO-1.

3.2 Catalytic performance of hydrothermally synthesized ceria for the methane combustion

A homogeneous gas phase reaction of CH_4 and O_2 was performed in order to determine an acceptable range of temperature. The compositions of the gases were the same as that used in ceria-catalyzed combustion test. The temperature was raised from 298 to 1,273 K at a heating rate of 10 K/min. **Figure 4** shows the mass count profiles of CO, H_2O and CO_2 produced by the oxidation of CH_4 by O_2. When the temperature was leached at around 933 K, the formation of these gasses began. No formation of any gasses was observed under 933 K since methane is one of the simplest and most stable of organic molecules, so the temperature of 933 K was insufficient to break the C–H bond. Based on these results, the ceria catalyzed reaction at 923 K had no influence on the homogeneous gas phase reaction.

The catalytic performance of CH_4 combustion over the ceria catalyst was evaluated via O_2 conversion. **Figure 5** compares the O_2 conversion after 30 and 270 min of CH_4 combustion at 923 K for each form of ceria. HSA Ceria maintained the O_2 conversion at around 94% even after 270 min. On the other hand, LSA Ceria and JRC-CEO-1 showed 92.1 and 88.2% at 30 min, and 91.5 and 86.4% at 270 min, respectively. The JRC-CEO-1 showed particularly poor stability in the O_2 conversion with time that compared to other ceria catalysts. Based on these results, CH_4 combustion performance varied with the type of ceria catalyst, and the HSA Ceria provided the highest and most stable level of catalytic activity. In this activity test, tendency of CH_4 conversion with type of ceria was very similar than that of O_2 conversion. Carbon mass balance well accorded at 100 ± 10% by the CH_4 conversion and the CO + CO_2 yield.

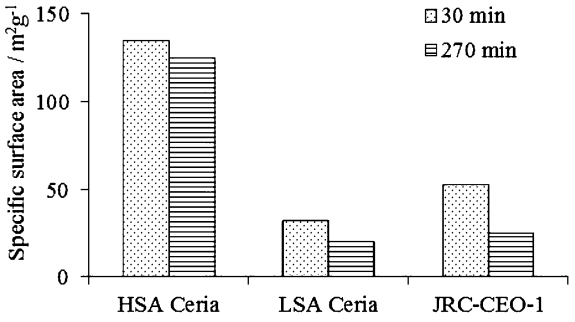

Fig. 6. Specific surface area after 30 and 270 min of ceria catalyzed CH_4 combustion at 923 K over HSA Ceria, LSA Ceria and JRC-CEO-1.

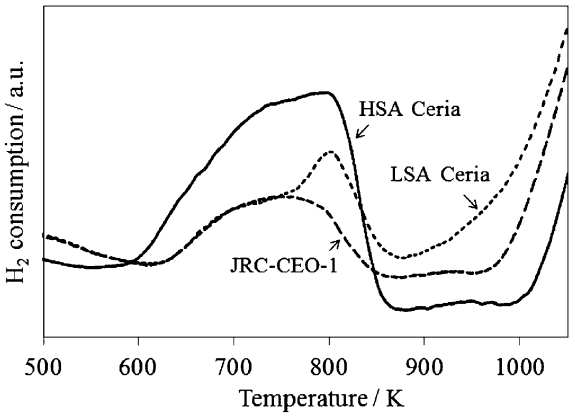

Fig. 7. H_2-TPR profile of HSA Ceria, LSA Ceria and JRC-CEO-1 after activity test.

The influential properties that ceria exerts on CH_4 combustion performance and the reasons for the highest level of catalytic activity for HSA Ceria are discussed here using the characteristics of BET-specific surface area, and H_2-TPR, TG, and IR analysis. The values for specific surface area of ceria after 30 and 270 min of activity test are shown in **Fig. 6**. HSA Ceria maintained a high and stable specific surface area at around 130 m^2/g during the activity test. LSA Ceria had much smaller levels of specific surface area at 32 and 20 m^2/g after 30 and 270 min of the activity test, respectively. JRC-CEO-1 also showed drastic decrease in specific surface area to 53 m^2/g after 30 min and finally reached at 25 m^2/g after 270 min. Based on these results, only HSA Ceria showed both a high and a very stable specific surface area, so this would be a main reason for its high catalytic activity over a long duration. In comparison with LSA Ceria and JRC-CEO-1, even though JRC-CEO-1 maintained a higher specific surface area compared with LSA Ceria, the O_2 conversion was opposite, which suggests the presence of another influential property on CH_4 combustion.

When either ceria or material that contains it is used as a catalyst for a combustion reaction of alkane, its OSC provides active oxygen and is an important factor for the improvement of the reactivity.[11] In order to evaluate the OSC of the ceria, H_2-TPR was applied and the profile of each ceria after a combustion test is indicated in **Fig. 7**. HSA Ceria demonstrated larger H_2 consumption that was associated with a reduction in Ce^{4+} on the ceria surface within a range of temperatures from 590 to 870 K. Both LSA Ceria and JRC-CEO-1 revealed similar TPR profiles at temperatures up to 750 K, but LSA Ceria showed a larger level of H_2 consumption at temperatures above 750 K compared with that of JRC-CEO-1. Since the CH_4 combustion test was conducted at 923 K for this study, the area obtained at both the baseline and the H_2-TPR profiles can be assumed to be the OSC that influenced on the catalytic activity. These results clearly showed that the HSA Ceria had more than twice OSC up to 923 K, compared with other ceria catalysts. This high OSC was associated with a reduction in the Ce^{4+} on the surface and should be correlated with the high specific surface area that leads to high combustion activity. LSA Ceria showed an OSC that was higher than that of JRC-CEO-1. This could be a main reason for the higher catalytic activity of LSA Ceria compared with that of JRC-CEO-1, although JRC-CEO-1 maintained a higher specific surface area. This result indicates that JRC-CEO-1 contained negative factors that reduced its OSC. As summarized by the TG and IR analysis in a previous report,[12] only JRC-CEO-1 contained a small percentage of cerium carbonate on the ceria surface, and the carbonate couldn't be decomposed at 923 K even under oxygen-rich conditions. The cerium species containing carbonate was maintained as a trivalent, which did not assimilate on OSC during the CH_4 combustion test. Hence, a key reason for the poor combustion activity of JRC-CEO-1 might come from the presence of a small percentage of cerium carbonate on the surface.

In summary, CH_4 combustion activity at 923 K was influenced by the specific surface area and OSC of the ceria catalyst used. HSA Ceria had high and stable level of specific surface area, and also maintained a high level of OSC even after 270 min of the activity test, which resulted in a high level of CH_4 combustion performance for a long duration. The LSA Ceria held a much lower specific surface area compared with that of the HSA Ceria and a low OSC that caused lower level of combustion activity. JRC-CEO-1 contained a small percentage of carbonate on the surface, which had a negative influence on the OSC. This poor OSC and low thermal stability of the specific surface area led to the lowest level of CH_4 combustion performance.

However, although HSA Ceria showed more than twice the specific surface area and the OSC compared to two references, all ceria showed over 85% in O_2 conversion with no significant difference. This suggested that the temperature of the CH_4 combustion was too high to differentiate the ceria properties in the combustion performance because this temperature might correspond to diffusion controlled region. In order to determine influence of temperature, CH_4 combustion over the ceria catalysts was conducted from 773 to 923 K at a heating rate of 10 K/min. Other condition was the same than that in the previous combustion test at 923 K. O_2 conversion with temperature is displayed in **Fig. 8**. In the range of low temperature from 773 to around 830 K, HSA Ceria and JRC-CEO-1 showed much higher O_2 conversion than LSA Ceria. Since specific surface area of HSA Ceria, LSA Ceria and JRC-CEO-1 after pretreated at 773 K for 1 h under an O_2 flow were 137, 54 and 134 m^2/g, respectively, much low catalytic activity of LSA Ceria seemed to be due to its low specific surface area. The difference in the O_2 conversion between HSA Ceria and JRC-CEO-1 was gradually increased with temperature. This also might be resulted from low thermal stability in specific surface area of JRC-CEO-1. Hence, catalytic activity in this range of temperature related to the specific surface area of the catalysts, meaning surface reaction controlled region. At over 830 K, O_2 conversion of LSA Ceria drastically increased and leached to the same level than that of HSA Ceria and JRC-CEO-1. From the results of specific surface area of the catalysts after the pretreatment and after 30 min of CH_4 combustion at 923 K, specific surface area of the catalysts over 830 K should much different and was decreased in the order HSA Ceria, JRC-CEO-1 and LSA

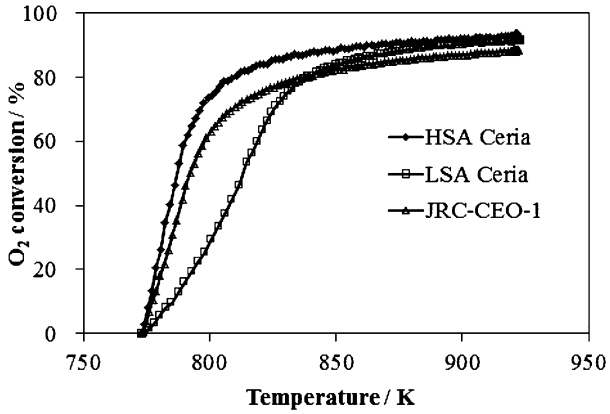

Fig. 8. O_2 conversion with temperature of ceria catalyzed CH_4 combustion from 773 to 923 K over HSA Ceria, LSA Ceria and JRC-CEO-1.

Ceria. This result shows that specific surface area of catalyst had limited impact on CH_4 combustion activity at over 830 K corresponding to diffusion controlled region.

4. Conclusions

Ceria with a high thermal stability was prepared via the thermal hydrolysis. This ceria was constructed with high crystallinity and high meso-porosity, resulting in an inhibition of sintering by calcination and in the maintenance of high level of specific surface area even after extensive ageing. This material was tested by CH_4 combustion at 923 K and showed higher catalytic performance even after 270 min compared with other ceria samples. This high activity was achieved because of high levels of stability and durability in the specific surface area and in the OSC. CH_4 combustion over ceria with temperature from 773 to 923 K also was tested. This revealed that combustion activity up to around 830 K related to the specific surface area of the ceria corresponding to surface-reaction-controlled region. At over 830 K, no significant difference in the activity was observed even much difference in the specific surface area of the catalysts. Hence, high temperature over 830 K corresponded to diffusion-controlled region.

It has been very difficult to utilize ceria for catalytic applications performed at high temperature because of its poor thermal stability that resulted in a limited number of active sites on the surface. In this study, however, we successfully synthesized ceria that had high thermal stability and demonstrated high catalytic activity at high temperatures. This developed material should open new windows for the utility of ceria over a wide range of temperatures in catalytic applications.

References

1) A. Beste and S. H. Overbury, *J. Phys. Chem. C*, **119**, 2447–2455 (2015).
2) A. Trovarelli, C. Leitenburg, M. Boaro and G. Dolcetti, *Catal. Today*, **50**, 353–367 (1999).
3) Q. Dai, H. Huang, Y. Zhu, W. Deng, S. Bai, X. Wang and G. Lu, *Appl. Catal., B*, **117–118**, 360–368 (2012).
4) A. Bueno-López, *Appl. Catal., B*, **146**, 1–11 (2014).
5) R. Jain and R. Maric, *Appl. Catal., A*, **475**, 461–468 (2014).
6) A. Igarashi, N. Ichikawa, S. Sato, R. Takahashi and T. Sodesawa, *Appl. Catal., A*, **300**, 50–57 (2006).
7) J. Zhang, H. Kumagai, K. Yamamura, S. Ohara, S. Takami, A. Morikawa, H. Shinjoh, K. Kaneko, T. Adschiri and A. Suda, *Nano Lett.*, **11**, 361–364 (2011).
8) L. A. Bruce, M. Hoang, A. E. Hughes, H. Terence and W. Turney, *Appl. Catal., A*, **134**, 351–362 (1996).
9) Y. Kamimura, M. Shimomura and A. Endo, *J. Colloid Interface Sci.*, **436**, 52–62 (2014).
10) D. Terribile, A. Trovarelli, C. d. Leitenburg and G. Dolcetti, *Chem. Mater.*, **9**, 2676–2678 (1997).
11) S. Pengpanich, V. Meeyoo, T. Rirksomboon and K. Bunyakiat, *Appl. Catal., A*, **234**, 221–233 (2002).
12) N. Ohtake, Y. Yamane, K. Nakagawa, M. Katoh and S. Sugiyama, *J. Chem. Eng. Jpn.*, **49**, 197–203 (2016).